## Title

AAV9-mediated Expression of a Non-self Protein in Nonhuman Primate Central Nervous System Triggers Widespread Neuroinflammation Driven by Antigen-presenting Cell Transduction



## Journal

Molecular Therapy, 22(2)

## ISSN

1525-0016

## Authors

Samaranch, Lluis
San Sebastian, Waldy
Kells, Adrian P
et al.

## Publication Date

2014-02-01

## DOI

10.1038/mt.2013.266

Peer reviewed

# AAV9-mediated Expression of a Non-self Protein in Nonhuman Primate Central Nervous System Triggers Widespread Neuroinflammation Driven by Antigen-presenting Cell Transduction

Lluis Samaranch[1], Waldy San Sebastian[1], Adrian P Kells[1], Ernesto A Salegio[1,3], Gregory Heller[1], John R Bringas[1], Philip Pivirotto[1], Stephen DeArmond[2], John Forsayeth[1] and Krystof S Bankiewicz[1]

*[1]Department of Neurological Surgery, University of California San Francisco, San Francisco, California, USA; [2]Department of Pathology and Laboratory Medicine, University of California San Francisco, San Francisco, California, USA; [3]Current address: Department of Neurological Surgery, Laboratory for CNS Repair, Brain and Spinal Cord Injury Center, University of California San Francisco, San Francisco, California, USA*

Many studies have demonstrated that adeno-associated virus serotype 9 (AAV9) transduces astrocytes and neurons when infused into rat or nonhuman primate (NHP) brain. We previously showed in rats that transduction of antigen-presenting cells (APC) by AAV9 encoding a foreign protein triggered a full neurotoxic immune response. Accordingly, we asked whether this phenomenon occurred in NHP. We performed parenchymal or intrathecal infusion of AAV9 encoding green fluorescent protein (GFP), a non-self protein derived from jellyfish, or human aromatic L-amino acid decarboxylase (hAADC), a self-protein, in separate NHP. Animals receiving AAV9-GFP into cisterna magna (CM) became ataxic, indicating cerebellar pathology, whereas AAV9-hAADC animals remained healthy. In transduced regions, AAV9-GFP elicited inflammation associated with early activation of astrocytic and microglial cells, along with upregulation of major histocompatibility complex class II (MHC-II) in glia. In addition, we found Purkinje neurons lacking calbindin after AAV9-GFP but not after AAV9-hAADC delivery. Our results demonstrate that AAV9-mediated expression of a foreign-protein, but not self-recognized protein, triggers complete immune responses in NHP regardless of the route of administration. Our results warrant caution when contemplating use of serotypes that can transduce APC if the transgene is not syngeneic with the host. This finding has the potential to complicate preclinical toxicology studies in which such vectors encoding human cDNA's are tested in animals.

*Received 14 May 2013; accepted 15 November 2013; advance online publication 14 January 2014. doi:10.1038/mt.2013.266*

## INTRODUCTION

Gene therapy for neurological diseases based on viral vectors is a useful and powerful technology. Serotype 2 of the adeno-associated viral vector (AAV2) has been the vector of choice for neurological clinical trials due to its neuronal specificity and limited immune response.[1] However, its modest transduction levels and lack of nonneuronal transduction have also been perceived as limitations. For this reason, a number of groups are currently investigating other serotypes in order to characterize their individual properties. Of all, adeno-associated virus serotype-9 (AAV9) has excited much interest as a candidate vector for gene therapy in the central nervous system (CNS) because AAV9 can cross the blood–brain barrier[2,3] from the circulation and transduce both neurons and glia.[4] However, it should be noted that the issue of preexisting neutralizing antibodies is still salient in this context.[3–6]

More ominously perhaps, we recently demonstrated in rats that AAV9 can trigger an adaptive immune response with neuronal loss after parenchymal infusion.[7] We concluded in that study that AAV9 transduces antigen-presenting cells (APC) in the brain, indicated by perivascular lymphocytic infiltration and upregulation of the major histocompatibility complex class II (MHC-II) in glia. This in turn provokes a humoral immune response (anti-human aromatic L-amino acid decarboxylase (hAADC) antibodies) leading to prominent damage in transduced tissues. In a previous study, some years ago, we reported very similar findings with AAV1 encoding *Renilla* green fluorescent protein (GFP).[8] The immunotoxicity we encountered in that study was associated with the presence of high titers of anti-GFP antibodies, strong upregulation of MHC-II, and evidence of cell loss in transduced brain tissues.

These data, led us to investigate immune response in nonhuman primates (NHP) after AAV9 delivery. In the rat study,[7] we hypothesized that expression of a self-protein in APC directed by AAV9 transduction would not yield a cytotoxic immune response. Hence, in the present study, we infused AAV9 harboring a non-self protein (GFP) or AAV9 harboring a self-protein (hAADC) in two cohorts of NHP by parenchymal infusion or cisterna magna (CM) injection. Parenchymal infusion into putamen was performed by convection-enhanced delivery with magnetic resonance imaging (MRI) guidance to ensure optimal distribution of the infusate.[9,10] As in the rat study, we observed similar neurotoxicity in NHP. Moreover, this phenomenon was triggered regardless of the route of the administration (parenchymal or intrathecal). These findings suggest that preclinical development of AAV9 should be

*Correspondence: Krystof S Bankiewicz, Department of Neurosurgery, University of California San Francisco, 1855 Folsom Street, MCB, Room 226, San Francisco, California 94103, USA. E-mail: Krystof.Bankiewicz@ucsf.edu*

performed in animal models with a species-matched transgene. Moreover, the fact that GFP triggers a full cytotoxic immune response resulting in elimination of specific classes of brain cells, perhaps at different rates, should prompt a reevaluation of all AAV data in which GFP was used as a transgene, particularly under conditions where APCs are transduced and high levels of transgene expression are routinely obtained.

## RESULTS

### Long-term striatal expression of AAV9-driven GFP results in extensive necrosis and vessel infiltration

Seven adult NHP were included in this study (**Table 1**). We administered AAV9-GFP (55 µl, $1.09 \times 10^{13}$ vg/ml) into the right putamen of Cyn1 and Cyn2 animals by MRI-guided convection-enhanced delivery. In the left putamen, animals received AAV2-GFP (55 µl, $1.0 \times 10^{13}$ vg/ml) as a control vector. MR images obtained during the surgery showed correct placement of cannula and good coverage of both putamina as indicated by the MR contrast agent (gadolinium) coinfused with the vector (**Supplementary Figure S1a**). Three months after infusion, Cyn1 and Cyn2 were euthanized and brains harvested. Postmortem immunohistochemical analysis of GFP expression at the infusion site revealed well-contained expression of the transgene within both striata but a larger transduction area in the AAV9 site compared to the AAV2 site (**Figure 1a** and **Supplementary Figure S1a**). Stained areas within these structures corresponded well with the MRI signal during infusion (**Supplementary Figure S1a**) and, as previously described, the AAV9 hemisphere contained many GFP-positive neurons and glia (**Supplementary Figures S1b and S2**). Further analysis revealed transduction of microglia (**Supplementary Figure S1b**). Low-magnification analysis revealed histopathological signs (*i.e.*, striatal tissue disorganization) in both striata, but more drastically in the striatum that received AAV9-GFP(**Figure 1a**). An extensive necrotic area was found in the AAV9 hemisphere that corresponded

**Table 1 Summary of different route delivery infusions**

| | Parenchymal ($n = 2$) | | | Cisterna magna ($n = 4$) | | | Control |
|---|---|---|---|---|---|---|---|
| | GFP | | | GFP | | hAADC | ($n = 1$) |
| | Cyn1 | Cyn2 | Cyn3 | Cyn4 | Cyn5 | Cyn6 | CynC |
| Survival time (days) | 90 | 90 | 14 | 19 | 24 | 21 | — |
| Weight (kg) | 3.0 | 6.2 | 9.2 | 4.0 | 4.2 | 2.7 | 2.9 |
| Titer ($\times 10^{13}$ vg/ml) | 1.0/1.09[a] | 1.0/1.09[a] | 1.09 | 1.09 | 1.09 | 3.0 | — |
| Volume (ml) | 0.055[b] | 0.055[b] | 2 | 2 | 2 | 2 | — |
| Clinical symptoms | No | No | No | Yes | Yes | No | No |

(—), nonapplicable; GFP, green florescence protein; hAADC, human aromatic L-amino acid decarboxylase; vg, vector genomes.
[a]Parenchymal monkeys received AAV2-GFP in the left putamen ($1.0 \times 10^{13}$ vg/ml) and AAV9-GFP in the right putamen ($1.09 \times 10^{13}$ vg/ml). [b]Same volume was injected in each side.

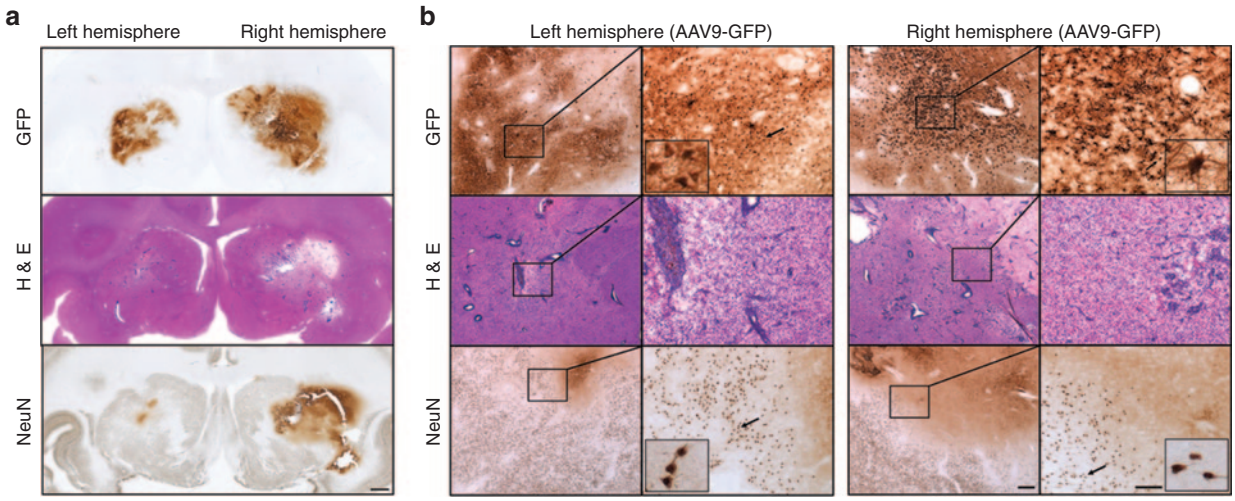


**Figure 1 Perivascular infiltration and neuronal loss after striatal infusion of AAV2-GFP (left) and AAV9-GFP (right).** Representative coronal nonhuman primate brain sections after receiving AAV2-GFP and AAV9-GFP in the left and right hemispheres, respectively. Greater transgene distribution was detected in the right hemisphere 90 days after parenchymal infusion (**a**, top). Corresponding with area of GFP transduction, H&E staining revealed larger tissue compromise in the AAV9 hemisphere than in the AAV2 side (**a**, middle). Accordingly, neuron-specific staining showed larger neuronal loss area on the right side (**a**, bottom). High-magnification analysis of transduced areas confirmed the neuron-specific tropism of AAV2 on the left side and the presence of GFP-positive neurons and astrocytes on the AAV9 hemisphere (**b**, top). Necrotic tissue and perivascular infiltration were present in both hemispheres, although more pronounced on the AAV9 side (**b**, middle). Detailed examination of NeuN immunostaining confirmed the absence of neurons, mainly in the AAV9-meidiated GFP-transduced area. Note that in the AAV2 side, the neuronal loss was mostly surrounding the infusion site (**b**, bottom). Bars = 1 mm for **a**; 500 µm for **b** low magnifications; 200 µm for **b** high magnifications (insets show digital magnifications of the areas pointed by arrows). AAV, adeno-associated virus; GFP, green fluorescent protein; H&E, hematoxylin and eosin.

with the GFP expression area, affecting not only most of the commissural putamen, but also ranging from the internal capsule dorsal to the infusion site and part of the caudate (**Figure 1a**). Higher-magnification analysis of hematoxylin and eosin (H&E)-stained sections revealed intense infiltration of inflammatory cells with a massive presence of reactive macrophages and lymphocytes, but no polynuclear leukocytes, as well as a generalized formation of perivascular cuffs (**Supplementary Figure S2a–c**). GFP expression was also visible in the contralateral AAV2-GFP–infused side that substantially covered the putamen (**Supplementary Figure S1a**). In accordance with the neuron-specific tropism of AAV2 previously described,[1,11] this hemisphere contained many GFP-positive neurons (**Figure 1** and **Supplementary Figure S2**). Although perivascular cuffing was also present in the putamen that received AAV2-GFP (**Figure 1** and **Supplementary Figure S3d**), tissue organization was not disrupted and there was less necrotic tissue than that seen in the AAV9-GFP–infused striatum.

Immunostaining with a neuron-specific marker (NeuN) evinced a dramatic reduction in the number of striatal neurons in the putamen that received AAV9-GFP, and a mild neuronal loss in the AAV2-GFP side (**Figure 1**). Beyond the injection site, some cortical areas (*i.e.*, premotor cortex) that project to the striatum were also devoid of, or showed downregulation of, NeuN immunostaining (**Supplementary Figure S3f**). This finding suggests that the damage/toxicity induced by AAV9-driven GFP expression in the putamen affected not only the primarily transduced site but also secondary regions in the brain, even in the contralateral hemisphere. Indeed, this evidence could explain the weak GFP expression that we found in some cortical regions. In addition, some GFP-positive round structures were present in these cortical regions, probably corresponding to degenerating either neuronal somas or processes (**Supplementary Figure S3e**). We also found GFP expression in other regions connected to the striatum such as the substantia nigra reticulata, which receives striatal projections, and also the substantia nigra pars compacta, which projects to the striatum (data not shown). The latter contained some GFP-positive neuronal cell bodies (soma), whereas the pars reticulata showed only GFP-positive fibers. No pathology was observed in either of these structures.

We also analyzed the inflammatory response by staining against some glial cell markers in both hemispheres. AAV9 putamen showed astrocytic transduction and a wide presence of immunoreactive astrocytes. Additionally, microglial cells were transduced and activated. Upregulation of MHC-II–positive cells surrounding the GFP-positive region in the AAV9-GFP putamen was also found and significant $CD8^+$ lymphocytic infiltration was present. A similar, but less intense, inflammatory response was found in the AAV2-GFP hemisphere. In that case, the tropism was strictly neuronal but astrocytes and microglia appeared activated. Accordingly, MHC-II was also upregulated and T-lymphocytic $CD8^+$ infiltration was present (**Figure 2a**,**b**). Although the striatal area with cellular toxicity was quite extensive on the AAV9-GFP side and mild in the AAV2-GFP side, no neurological signs or behavioral adverse effects were observed in Cyn1 or Cyn2 animals.

Since AAV2 is a neuron-specific serotype in the brain and neurons are not professional APCs, we suspected that the modest toxicity seen in the AAV2-GFP hemisphere was mediated by the adaptive immunity generated by AAV9 in the other hemisphere. To confirm that AAV2-GFP could not generate an adaptive response on its own, we performed the same immunohistochemical staining in one of our historical control animals that had received only a single parenchymal injection of AAV2-GFP under the same experimental conditions. In agreement with previous data indicating the benign effects of AAV2-GFP,[2,3,12] we found that this animal showed only a slight immune reaction, basically located at the injection area, most likely caused by innate immune activation from tissue disruption after injection (**Supplementary Figure S4**). In comparison, Cyn1 and Cyn2 showed an extensive and well-established immune reaction in their AAV2-injected side (left hemisphere). In addition, by immunoblot analysis, humoral response was confirmed by the presence of circulating anti-GFP antibodies in these two GFP-injected animals in comparison with the control animal (CynC; **Supplementary Figure S5**). Together with the absence of astrocytic transduction in the AAV2-injected hemisphere (**Figure 1**), these data suggest the presence of a robust systemic immune response driven primarily by AAV9-GFP transduction of glia that enabled a humoral response against neurons in the AAV2-GFP hemisphere presenting GFP antigens through neuronal MHC-I.

## Intrathecal delivery of AAV9-GFP but not AAV9-hAADC triggers inflammatory and immune responses

Previous experiments in NHP demonstrated that intrathecal delivery of AAV9 resulted in strong widespread expression of the transgene throughout white matter tracts and cerebellum.[4,13] However, subsequent studies in rats showed that parenchymal administration of AAV9-GFP resulted in transduction of not only neurons but also astrocytes, which are APC in the brain.[3–7] Furthermore, this ability of AAV9 to transduce APC in contrast to the neuron-specific tropism of AAV2, resulted in the mounting of an adaptive immune response against GFP.[7] Hence, we wondered whether broadly distributed CNS expression of GFP after intrathecal rather than more focal parenchymal delivery of AAV9-GFP could modify the response seen after parenchymal infusion in any way. To investigate this issue, we performed intrathecal injections into the CM of four NHP. We administered AAV9-GFP (2 ml, $1.1 \times 10^{13}$ vg/ml) to three animals (Cyn3-5) and to a fourth (Cyn6) we administered AAV9-hAADC (2 ml, $3.0 \times 10^{13}$ vg/ml), a self-recognized protein for primates (**Table 1**).

Our experiments in rats showed the strongest immune reaction 8 weeks after AAV9 delivery.[7,8] Thus, we planned short-term (2 weeks, Cyn3) and long-term (3 months, Cyn4 and Cyn5) survival groups. About 3 weeks after AAV9-GFP intrathecal administration, Cyn4 and Cyn5 presented serious adverse side effects such as low appetite, poor hand-eye coordination, impaired balance, and ataxia, which were suggestive of cerebellar damage. Consequently, animals were euthanized and brains harvested for histological assessment. Cyn3, the 2-week survival animal, did not show any neurological signs or adverse effect during follow-up. Cyn6, that received AAV9-hAADC (self-protein), also did not show any behavioral signs and was euthanized 3 weeks after the infusion in order to match the AAV9-GFP group.

Postmortem analysis of GFP expression in the brain revealed different transgene immunostaining with respect to survival time of the animals (**Supplementary Figure S6a**). Thus, Cyn4 and

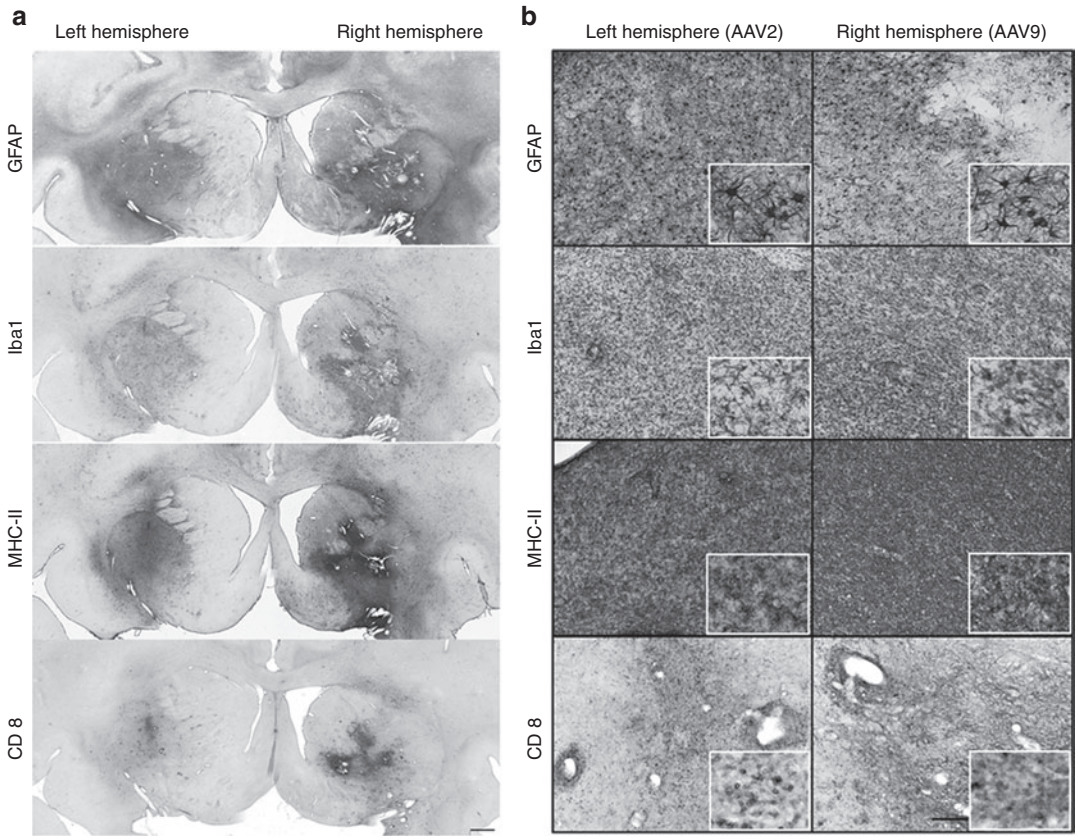


**Figure 2 Inflammatory response after putaminal CED infusion.** Consecutive coronal brain sections containing the cannula track in the putamen were stained for astrocytes (GFAP), microglia (Iba1), APC (MHC-II), and T-cytotoxic cells (CD8). Low magnification images show the extension of the putaminal immune reaction directed by activated astrocytes and microglia, upregulation of MHC-II and T-cytotoxic cells in both hemispheres, being it more dramatic on the (**a**) AAV9 side. Although there were differences in the extension and the intensity, detailed cellular analysis of representative sections showed strong activation of astrocytes in both hemispheres (**b**,*GFAP*) and the presence of hyperactive microglia clusters as well (**b**,*Iba1*). As a consequence of an innate reaction, the immune response was accompanied by a robust and global antigen conjugation with MHC-II (**b**, MHC-II) as well as T-cell cytotoxic infiltration (**b**,*CD8*). Bars = 1 mm for **a**; 200 µm for **b** (insets show digital magnifications). APC, antigen-presenting cells; CD8, cluster of differentiation 8α; GFAP, glial fibrillary acidic protein; GFP, green fluorescent protein; Iba1, ionized calcium-binding adaptor molecule; MHC-II, major histocompatibility complex-II.

Cyn5, euthanized 3 weeks after AAV9 delivery, showed broader transduction throughout both cerebellum and brain cortex. In contrast, Cyn3, which had the shortest survival time (2 weeks) and no side effects, evinced more restricted GFP distribution. Cyn6 brain sections were processed for hAADC immunostaining, and we observed an expression pattern very similar to that of the AAV9-GFP animals with the same survival time (3 weeks). Double fluorescent immunostaining confirmed that Purkinje cells were transduced in the cerebellum after CM delivery (**Supplementary Figure S6b**).

Since two of the AAV9-GFP animals developed serious deficits in motor coordination, we investigated a possible cerebellar histopathology. Cerebellar sections stained with H&E indicated non-pronounced cellular loss in the Purkinje layer (**Supplementary Figure S6c**), but no evidence of perivascular infiltration or luminal pathology in the blood vessels in the cerebellar cortex (**Supplementary Figure S6c**). Immunohistochemical analysis of the cerebellum revealed that ataxic animals (Cyn4 and Cyn5) suffered a dramatic depletion of the calcium-binding protein calbindin-D28k in Purkinje neurons, compared with the control (CynC), nonataxic AAV9-GFP (Cyn3), and AAV9-hAADC (Cyn6; **Figure 3**) animals. Interestingly, the 2-week survival animal (Cyn3) did not show cerebellar dysfunction, suggesting a clear time-dependent relation between GFP expression and motor impairment.

As we observed in a topological analysis, calbindin depletion correlated with regions that showed higher expression of GFP in the cerebellum (**Figure 4a**). In contrast, no cerebellar cell dysfunction was observed in the animals that received hAADC (**Figure 4b**). Since calbindin is a calcium-binding protein highly expressed in Purkinje cells, we conjectured that GFP expression in the cerebellum could explain (directly or indirectly) the absence of calbindin immunoreactivity and consequently, aberrant $Ca^{2+}$ homeostasis in the cells. These results accord with previous studies that correlated cellular obliteration of calbindin and lack of synaptic calcium-mediated signaling with motor impairment.[7,14] In addition, adjacent brain and cerebellar sections were stained against inflammatory markers. Staining for both glial fibrillary acidic protein (GFAP) and Iba1 revealed the presence of large numbers of activated astrocytes and microglia in the cerebellum 3 weeks after AAV9-GFP CM infusion (**Figure 5a**,**b**) compared to Cyn3, which was euthanized only 2 weeks after AAV9-GFP administration (**Figure 5a**,**b**). The latter still displayed an increased number of

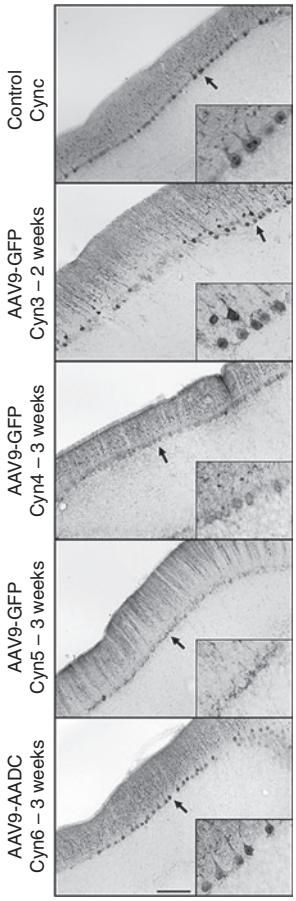


**Figure 3 Immunohistochemical analysis of Purkinje neuronal population in the cerebellum after AAV9 infusion into cisterna magna.** Representative sections of cerebellar cortex after AAV9-GFP (Cyn3, Cyn4, and Cyn5) or AAV9-hAADC (Cyn6) intrathecal injection stained for calbindin, a Purkinje neuron specific marker. Calbindin immunostaining revealed that monkeys with adverse motor effects (Cyn4 and Cyn5) also had Purkinje cell dysfunction as shown by the presence of Purkinje neurons lacking calbindin immunoreactive signal. In contrast, the animal that received AAV9-hAADC (Cyn6) did not show calbindin dysregulation in the cerebellum compared with the control animal (CynC). Interestingly, the 2-week survival animal (Cyn3) did not show cerebellar dysfunction. Bars = 500 µm (insets show digital magnifications of the areas indicated by arrows). AAV9, adeno-associated viral vector serotype 9; Cyn, cynomolgus; GFP, green fluorescent protein; hAADC, human amino acid decarboxylase.

activated glia compared to a naive control NHP (CynC). The morphology of glia (*i.e.*, enlarged bodies) indicated they were activated and they also displayed a disorganized topological distribution. In contrast, astrocytic and microglial staining in the AAV9-hAADC animal (Cyn6) showed a very similar presence and distribution of these cells to the control animal (**Figure 5a**,**b**).

AAV9-GFP and AAV9-hAADC expression was not as strong throughout the cerebral cortex as it was in the cerebellum. Even so, Cyn4 and Cyn5 showed glial cell activation in different regions of the occipital cortex in contrast to the control animal (CynC). Interestingly, cortical regions also revealed astrocytes and microglia activated after AAV9-hAADC (Cyn6) in comparison with the control, but weak compared with Cyn4 and Cyn5 as the other extreme of the range (**Supplementary Figure S7**). Although human AADC might be considered as a monkey self-recognized

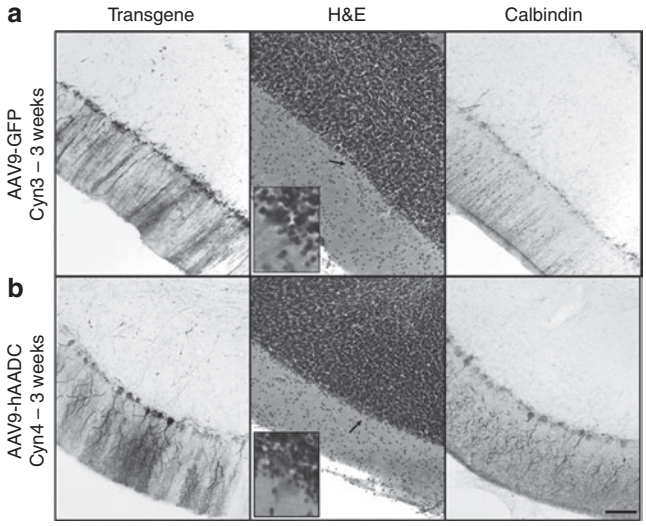


**Figure 4 Correlation of Purkinje cell dysfunction with GFP expression.** Analysis of cerebellar regions with high levels of GFP expression revealed dramatic depletion calbindin into the Purkinje cells in the animals that received AAV9-GFP. H&E and calbindin staining confirmed the absence of these cells. In contrast, Purkinje neurons were present in the cerebellum of the animal that received AAV9-hAADC as shown by H&E, as well as hAADC and calbindin staining. Bars = 500 µm (inset shows digital magnifications of the area indicated by the arrow).

protein in view of the close homology of *homo* (NP_001076440) and *macaca* (XP_001082132) AADC, sequence discrepancy between the two proteins, about 15 amino acids (97% homology), could have caused this mild immune reaction.

Because the reaction to AAV9-GFP was associated with loss of neurons and strong inflammation, we suspected a cell-mediated immune response. Such a response should be evident by upregulation of MHC-II after AAV9-GFP transduction. Accordingly, MHC-II immunostaining revealed an extensive presence of MHC-II–positive cells in the cerebellum and cortex 3 weeks after AAV9-GFP, but not after AAV9-hAADC intrathecal injection (**Figure 5c** and **Supplementary Figure S7**). In addition, as in the parenchymal delivery, animals after cerebrospinal fluid (CSF) GFP injection also exhibited circulating anti-GFP antibodies in ataxic AAV9-GFP NHP, but not in control, confirming the humoral immune reaction (**Supplementary Figure S5**).

Altogether, these data suggest that AAV9-mediated neuronal and glial cell transduction results in strong GFP expression that triggers a clearly progressive inflammatory reaction accompanied by a strong immune response against GFP. We conclude that this reaction underlies the dysfunction/degeneration of the loss of Purkinje neurons displayed by Cyn4 and Cyn5 animals 3 weeks after AAV9-GFP but not AAV9-hAADC administration, thereby explaining the neurological signs and ataxia.

## DISCUSSION

So far, our experience with AAV vectors for neurological applications both in animal experiments and clinical trials has served to build a high degree of confidence that, whatever the degree of therapeutic efficacy obtained, the safety of AAV-based gene therapy for neurological diseases is remarkable. Clinically, much of this safety record may be ascribed to the use of AAV2, a neurotropic

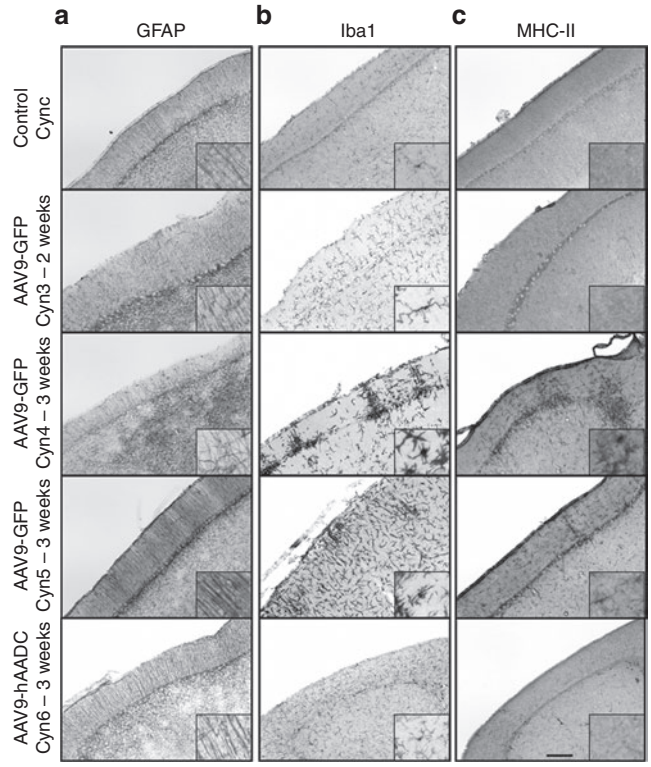


**Figure 5 Inflammatory response after CSF delivery into cisterna magna.** Coronal sections containing cerebellum were stained against GFAP (astrocyte marker), Iba1 (microglia marker) and MHC-II (APC marker). Animals that presented behavioral adverse effects and Purkinje neurons degeneration (Cyn4 and Cyn5) also showed an established immune response in the cerebellum 3 weeks after AAV9-GFP delivery. Activated glial cells (GFAP+) were found in the molecular layer of the cerebellar cortex in the ataxic monkeys in comparison with the control monkey (CynC) and the monkey that received (**a**) hAADC. As well, aggregates of immunoreactive microglia (**b**) and upreguation of MHC-II were found in the cerebellar cortex of these animals (**c**). Compared to the control animal, Cyn3 (2-week survival after AAV9-GFP delivery) and Cyn6 (3-week survival after AAV9-hAADC) did not show any signs of immune response. Bars = 500 µm for **a**, **b**, and **c** (inset shown digital magnifications). APC, antigen presenting cells; GFAP, glial fibrillary acidic protein; GFP, green fluorescent protein; Iba1, ionized calcium-binding adaptor molecule; MHC-II, major histocompatibility complex-II.

serotype, since neurons cannot trigger a cell-mediated immune response, although they can present antigen via MHC-I. As interest has grown in other serotypes, however, immunological dangers have come to the fore, and optimizing viral vectors to avoid immune response of the host remains an important challenge in this field. It has been postulated that route of application, target tissue, vector serotype, levels of expression, and even dose are determinant factors to establish the type of immune response.[9,10,15] In our experience, other aspects are also important, such as vector quality.

Most published studies directed at the question of immune response to vector have focused on the presence of neutralizing antibodies after administration in mammalian brain,[6,16,17] but few have addressed the problem of transducing APC in the CNS. In a previous study, we reported the propensity of AAV1 to trigger significant immune response in the primate brain through the transduction of APC.[8] This finding agrees with data from Dodiya *et al.* in which AAV1-eGFP infusion into the NHP putamen was associated with perivascular cuffing.[18–20] In our opinion, broad tropism is less likely to yield immunotoxicity when the transgene is syngeneic with the host, and immunity directed at non-self proteins may not be easily detected in short-term experiments.

In our hands, highly efficient transduction with vectors such as AAV9 yielded unmistakable evidence of immunotoxicity. In a previous study in rodents,[7] we showed for the first time that AAV9-mediated expression of a human protein, hAADC, in rat striatum triggered a dramatic cell-mediated and humoral response when AAV9 was used to drive AADC expression, in stark contrast to the situation with AAV2-hAADC. In some ways, the more disturbing finding was that AAV9-GFP also triggered a similar, although less dramatic, response. GFP is one of the most widely used synthetic reporter genes in this field and, even though it is not even a mammalian protein, it is generally regarded as benign. Clearly, the use of GFP to assess cellular tropism can be complicated if transduced cells are being eliminated before they can be detected. It is difficult to imagine how GFP can be considered an acceptable control vector under such circumstances.

In the present study, we extended our studies to NHP and examined two routes of vector delivery to the CNS: parenchymal and intrathecal. Just as we observed in rodents, AAV9-driven, but not AAV2-mediated, expression of GFP provoked inflammation, tissue necrosis, and immune activation after parenchymal (putaminal) infusion. However, since this experiment involved infusion of AAV2-GFP into one hemisphere and AAV9-GFP into the other, we could also observe whether immune response to AAV9-GFP resulted in response to AAV2-GFP–mediated transduction. It should be noted that we have never seen any neuropathological reaction to AAV2-GFP in NHP in many independent studies (see also **Supplementary Figure S4**). Interestingly, in the present study, some blood vessel cuffs/white blood cell infiltration could be seen by H&E staining in the AAV2-GFP infused putamen, although slight by comparison to the reaction seen in the AAV9 hemisphere. The absence of transduced astrocytes in the AAV2-injected hemisphere confirms the neuron-specific tropism of AAV2. We think that the unexpected gliosis as well as the upregulation of MHC-II and the presence of lymphocytes suggest that the inflammatory reaction was a AAV9-mediated response, in which the expression of the non-self protein GFP in APC transduced by AAV9 presented MHC-II–conjugated GFP peptides on their surface, thereby activating a classic adaptive immune response. This presentation caused the proliferation of T-cells cytotoxic $CD8^+$ that react against GFP both in the right side (AAV9-mediated) and in the left side (AAV2-mediated) and also stimulation of B cells and production of antibodies against GFP. This phenomenon no doubt underlies the loss of NeuN-expressing cells not only in the AAV9-GFP–infused putamen, but also in motor cortical areas known to send projections to striatum. Clearly, retrograde transport of AAV9-GFP from the primary injection site may recruit secondary sites into the pathological immune response.

We also investigated immunological implications of the intrathecal route of delivery of AAV9 vector. We have recently demonstrated that AAV9 is very efficient when infused in the CM of NHP.[4,13] As in the prior study, the present report revealed a broad cellular tropism of AAV9 in both brain cortex and cerebellum. To

our surprise, in this second study, the intended long-term follow-up group had to be euthanized only 3 weeks after infusion due to the appearance of adverse neurological effects, chiefly ataxia. In contrast, animals in the previous intrathecal study did not show any adverse effects after the same period of follow-up. The basis of this difference is obscure at present, but we have noticed a significant dose effect of AAV9-GFP on the toxicity of the immune response that may be in turn driven by the absolute number and type of transduced APC and the strength of the promoter driving GFP expression. Currently, we do not have a simple explanation for this discrepancy, but the most obvious difference between the two experiments lies in the fact that the earlier study used AAV9 with a modified chicken β-actin promoter to direct GFP expression, whereas the present study employed a cytomegalovirus promoter. It has been reported that cytomegalovirus promoter is stronger than chicken β-actin promoter in AAV, and even a relatively modest difference in expression may result in a significantly faster and more profound pathology.[21] This is an issue that we intend to explore more fully in a future study.

In the intrathecal assessment, the severe deficits in motor coordination in the AAV9-GFP animals was associated with a cellular depletion or robust cerebellar lesion, most probably in the spinocerebellum (vermis and paravermis) and the vestibulocerebellum (flocculonodular lobe), closest to the injection site, the CM. Interestingly, standard H&E histological staining of the cerebellar cortex revealed the apparent presence of Purkinje cells in the cellular layer of the cerebellum. In contrast, calbindin immunostaining evinced a dramatic reduction of immunoreactivity in cerebellar areas with high levels of GFP expression. These results are consistent with the phenotype exhibited by a Purkinje cell-specific calbindin null mutant mouse (*Calb$^{tm2}$/L7Cre-2*).[14] As with our animals, these Purkinje calbindin-deficient mice exhibit a prominent coordination impairment that could not be restored by any plasticity mechanism or prolonged training. Calbindin is essential to $Ca^{2+}$ buffering in Purkinje cells. Thus, we postulate that GFP may cause an aberrant $Ca^{2+}$ homeostasis in the cells by strongly downregulating calbindin expression, consequently dysregulating synaptic calcium-mediated signaling and adversely affecting motor function. Although, further experiments to evaluate $Ca^{2+}$ buffering directly in this neurons are necessary, this is not the first time we have seen this phenomenon. AAV1-GFP was equally capable of eliciting as great a downregulation of GFAP in striatal astrocytes, even though the astrocytes themselves remained intact.[8] We surmise that optimization of GFP translation over the years has resulted in a reporter that can compete significantly with translation of abundant cytoplasmic proteins.

Nevertheless, this issue emphasizes the point made above regarding the assessment of expression of a reporter gene that triggers immunopathology in a somewhat dose-dependent way. Clearly, however, this problem is only encountered with foreign antigens. Intrathecal AAV9-hAADC transduced the same repertoire of brain cells as AAV9-GFP but induced no cerebellar pathology or inflammation. Nevertheless, although hAADC did not elicit an immune response, microgliosis was present in the cortex with the absence of astrocyte activation and MHC-II upregulation. The fact that human and monkey AADC proteins are not identical (97% homology) could underlie the mild Iba1 gliosis in the cortex.

In summary, our results suggest that the most appropriate reporter gene, therefore, would be a nonfunctional version of a protein that is otherwise syngeneic with the host, but is not normally expressed in the target organ. Our findings raise some safety concerns regarding the use of AAV9, or any other vector capable of transducing APC, for gene therapy. First, APC transduction potentially complicates preclinical toxicology studies in which non-self proteins are being expressed at a level sufficient to trigger T-cell priming. Thus, in US Food and Drug Administration (FDA)-mandated good laboratory practice (GLP) toxicology studies, an AAV9 vector directing expression of a human protein could generate spurious neurotoxicity that would strongly compromise toxicological data and mislead investigators. Similarly, use of transgenes that are considered foreign proteins to mammals, such as tetracycline transactivator, could be entirely unacceptable for both preclinical and clinical development. However, such issues must be addressed for each vector construct under study. We should also be cautious when using such vectors for diseases caused by the complete lack of a protein or its naive isoform. Delivering a protein that has never been expressed by a patient before, even if it is a human self-protein, could be problematic since the immune system might not recognize it as a self-protein. Overall, we emphasize that our findings in rodents and NHP do not preclude the use of AAV vectors that transduce APC in the CNS, but counsel caution when delivering such vectors harboring non-self proteins, as would be the case of GLP toxicological preclinical studies in animal models or clinically.

## MATERIALS AND METHODS

***Animals.*** A total of seven adult Cynomolgus macaques (*Macaca fascicularis*; ~3.0–9.0 kg) were included in this study (**Table 1**). Two (Cyn1 and Cyn2) were infused in the striatum and 4 (Cyn3-6) were injected intrathecally into the CM. In addition, one more animal (CynC) received no parenchymal/CSF infusion and was included as a control.

Animals were tested for the presence of anti-AAV antibodies as previously described and all were seronegative with antibody titers of <1:100.[22] Qualified veterinary personnel monitored all the animals daily throughout the study. Since a possible immune reaction to AAV-GFP expression was expected, all animals were closely observed after AAV delivery until the end of the study. Planned survival time was 3 months after AAV delivery for all the animals, except for the CynC control animal that did not undergo receive AAV and was euthanized soon after its arrival at UCSF animal facilities. All procedures were carried out in accordance with the UCSF Institutional Animal Care and Use Committee (San Francisco, CA) and at Valley Biosystems. (Sacramento, CA).

***Vector production.*** As previously described,[23,24] the hAADC and GFP cDNA were cloned into either an AAV9 (AAV9-hAADC or AAV9-GFP) or an AAV2 (AAV2-GFP) shuttle plasmid, and viral particles of recombinant AAV9 or AAV2 containing either hAADC or GFP under the control of the cytomegalovirus promoter were manufactured by the Research Vector Core at Children's Hospital of Philadelphia by standard helper-free transfection method (three-plasmid transfection).[23] Vectors were purified from cell extracts by CsCl centrifugation and concentrated to $\sim 3.0 \times 10^{13}$ (AAV9-hAADC), $1.0 \times 10^{13}$ (AAV2-GFP), and $1.09 \times 10^{13}$ (AAV9-GFP) vector genomes/ml. For parenchymal infusion, a MR-compatible tracer, gadolinium (2 mmol/l, Prohance; Bracco Diagnostics,

Monroe Township, NJ) was added to the vector preparation in order to visualize delivery by MRI.[25]

### *Vector delivery*

***Brain parenchyma.*** Two monkeys (Cyn1 and Cyn2) received an infusion of AAV9-GFP and AAV2-GFP into the right and left putamen, respectively, by means of real-time guided convection-enhanced delivery.[9,10] Briefly, animals were placed supine in a MRI-compatible stereotactic frame and, after craniotomy, underwent stereotactic placement of MR-compatible, skull-mounted, temporary cannula guides over each hemisphere. NHP were then moved into the MRI (3T Magnetom Trio, Siemens Healthcare Global, Germany) to calculate the trajectory to the putamen inside the brain. Once the trajectory was set, a ceramic custom-designed fused silica reflux-resistant cannula with a 3-mm stepped tip was used for the infusion.[25,26] Animals received ~55 µl of either AAV9-GFP or AAV2-GFP into right and left putamen, respectively. Infusion rate was ramped up to a maximum of 3 µl/minute. Once the infusion ended, guide devices were removed from skull and animals were taken back to their home cages and monitored during recovery from anesthesia.

***CM.*** Four NHP (Cyn3-6) were injected into the CM as described previously.[4] Briefly, after induction of deep anesthesia, animal was placed in lateral decubitus position and a 22G spinal needle attached to an IV line and a 3-ml syringe was manually guided into the CM. Once the needle was inside the CM, the correct location was verified by aspiration of a small volume of CSF and 2 ml of either AAV9-GFP vector (Cyn3-5) or AAV9-hAADC (Cyn6) were manually delivered at 1 ml/minute into the CSF. After injection, each animal was closely monitored during recovery from anesthesia.

Since a possible immune reaction to AAV-GFP expression was expected, all animals were observed daily after AAV delivery until the end of the study. Planned survival time was 3 months after AAV delivery for all the animals, except for the CynC control animal that did not undergo any AAV delivery and was euthanized soon after its arrival to UCSF animal facilities.

Historical control animal was used for the AAV2-GFP vector injections. All the vectors were produced under the same manufacturing process and quality control assays. Parenchymal deliveries were performed by identical surgical technique and experimental parameters of infusion rate.

***Tissue collection and processing.*** Animals were transcardially perfused with phosphate-buffered saline (PBS) followed by 4% paraformaldehyde/PBS. Brains were harvested, sliced into 6-mm coronal blocks in a brain matrix, postfixed by immersion in 4% paraformaldehyde/PBS overnight, and then transferred to 30% (w/v) sucrose. A sliding microtome was used to cut serial 40-µm sections for histological processing. All sections were stored in cryoprotectant solution until further use.

In order to assess transgene expression, we performed immunohistochemistry with polyclonal antibodies against either GFP (rabbit anti-GFP, 1:1,000; G10362 Molecular Probes, Life Technologies, Foster City, CA) or hAADC (rabbit anti-DOPA decarboxylase (DDC), 1:1,000; AB136 Millipore, Temecula, CA). Tissue sections were washed in PBS, endogenous peroxidase activity blocked in 1% $H_2O_2$/30% alcohol/PBS, and then rinsed in PBST (PBS/1% Tween 20). Sections were then incubated in Background Sniper blocking solution (BS966G; Biocare Medical, Concord, CA) followed by a 24-hour incubation at 4 °C with primary antibody against either GFP or DDC in Da Vinci Green diluent (PD900; Biocare Medical). The next day, sections were washed in PBST and incubated in Rabbit Mach 2 HRP-polymer (RP531L; Biocare Medical) at room temperature for 1 hour. All sections were chromogenically developed with 3,3′-diaminobenzidine (DAB) (DAB Peroxidase Substrate Kit, SK-4100; Vector Laboratories, Burlingame, CA) according to the manufacturer instructions. To study immune response, antibodies against neurons (anti-NeuN, mouse monoclonal, 1:300; MAB377 Millipore), GFAP (mouse anti-GFAP, 1:100,000; MAB360 Millipore), ionized calcium binding adaptor molecule 1 (Iba1; rabbit anti-Iba1, 1:1,000; CP290C Biocare Medical) the MHC-II (mouse anti-MHCII; 1:300; M3887-30 US Biological , Salem, MA) and cluster of differentiation 8α (CD8α; mouse anti-CD8, 1:100; MCA4609T AbD-Serotec, Bio-Rad Life Science, Hercules, CA) were used separately following the immunoperoxidase staining protocol described above. In addition, immunohistochemistry of representative sections of all animals were stained for calbindin (Cb; rabbit anti-Cb, 1:100,000; CB-38a Swant, Switzerland) a widely recognized marker of Purkinje cells.

A standard H&E staining was carried out in all animals in order to assess possible pathological signs. Briefly, slide-mounted sections were washed in graded alcohol (100, 95, and 70% v/v; 3 minutes each), rehydrated in distilled water and stained in hematoxylin (3 minutes; Leica Microsystems, Wetzlar, Germany). After sections were washed, they were differentiated in 0.5% glacial acetic acid/70% alcohol, immersed in bluing solution, and counterstained in eosin (2 minutes; Leica Microsystems). Finally, after washing them a final time, sections were dehydrated in alcohol (95 and 100%; 3 minutes each), immersed in fresh xylene (2×3 minutes), and preserved under coverslips. H&E sections were blindly analyzed by a board-certified pathologist (S.D.).

***Immunoblot assay.*** Antibodies against GFP were measured by semiquantitative blotting analysis as described previously.[8] Briefly, 100 ng of synthetic GFP protein (GR86835; Abcam, Cambridge, MA) was added and dried on a wet nitrocellulose membrane (162-0117; Bio-Rad, Hercules, CA) as the antigen solution assigned. Serum was extracted from total blood in each animal at the necropsy day and immediately frozen on dry ice. Immunoblot was performed with a Bio-Dot SF Microfiltration apparatus (170-6542; Bio-Rad) following manufacturer protocol on serial dilutions of sera as 1:100, 1:400, 1:1,600, and 1:6,400. Horseradish peroxidase–conjugated goat anti-monkey IgG Peroxidase (60R-IG020HRP; Fitzgerald, North Acton, MA) was used as secondary antibody at 1:5,000 dilution, and color development of enzyme-conjugated antibodies were performed by Immun-Blot Opti-4CN Colorimetric kit (170-8235; Bio-Rad). A serum from naive money (CynC) was used as negative control.

## ACKNOWLEDGMENTS

This study was supported by a grant to K.S.B. from NIH-NINDS (R01NS073940-01). L.S. is a recipient of the Edward M. Schuchman Research Fellowship from the National Niemann-Pick Disease Foundation. No competing financial interests exist.

## SUPPLEMENTARY MATERIAL

**Figure S1.** Overlapping of MR imaging and the GFP expression after AAV9 and AAV2 parenchymal delivery.
**Figure S2.** Differences in the morphology of the transduced cells after AAV2 and AAV9 injections into the putamen.
**Figure S3.** Neuropathologic landmarks three months after parenchymal injection of AAV9-GFP.
**Figure S4.** Control AAV2-GFP animal injected into the thalamus.
**Figure S5.** Transgene distribution after AAV9 injection into cisterna magna.
**Figure S6.** Immune response in the brain cortex after CSF delivery of either AAV9-GFP or AAV9-hAADC.
**Figure S7.** Neurotoxic effect through humoral immunity.

## REFERENCES

1. Forsayeth, JR, Eberling, JL, Sanftner, LM, Zhen, Z, Pivirotto, P, Bringas, J *et al.* (2006). A dose-ranging study of AAV-hAADC therapy in Parkinsonian monkeys. *Mol Ther* **14**: 571–577.
2. Foust, KD, Nurre, E, Montgomery, CL, Hernandez, A, Chan, CM and Kaspar, BK (2009). Intravascular AAV9 preferentially targets neonatal neurons and adult astrocytes. *Nat Biotechnol* **27**: 59–65.
3. Gray, SJ, Matagne, V, Bachaboina, L, Yadav, S, Ojeda, SR and Samulski, RJ (2011). Preclinical differences of intravascular AAV9 delivery to neurons and glia: a comparative study of adult mice and nonhuman primates. *Mol Ther* **19**: 1058–1069.
4. Samaranch, L, Salegio, EA, San Sebastian, W, Kells, AP, Foust, KD, Bringas, JR *et al.* (2012). Adeno-associated virus serotype 9 transduction in the central nervous system of nonhuman primates. *Hum Gene Ther* **23**: 382–389.

5. Haurigot, V, Marcó, S, Ribera, A, Garcia, M, Ruzo, A, Villacampa, P, *et al.* (2013). Whole body correction of mucopolysaccharidosis IIIA by intracerebrospinal fluid gene therapy. *J Clin Invest* **123**: 3254–3271.
6. Gray, SJ, Nagabhushan Kalburgi, S, McCown, TJ and Jude Samulski, R (2013). Global CNS gene delivery and evasion of anti-AAV-neutralizing antibodies by intrathecal AAV administration in non-human primates. *Gene Ther* **20**: 450–459.
7. Ciesielska, A, Hadaczek, P, Mittermeyer, G, Zhou, S, Wright, JF, Bankiewicz, KS *et al.* (2013). Cerebral infusion of AAV9 vector-encoding non-self proteins can elicit cell-mediated immune responses. *Mol Ther* **21**: 158–166.
8. Hadaczek, P, Forsayeth, J, Mirek, H, Munson, K, Bringas, J, Pivirotto, P *et al.* (2009). Transduction of nonhuman primate brain with adeno-associated virus serotype 1: vector trafficking and immune response. *Hum Gene Ther* **20**: 225–237.
9. Bankiewicz, KS, Eberling, JL, Kohutnicka, M, Jagust, W, Pivirotto, P, Bringas, J *et al.* (2000). Convection-enhanced delivery of AAV vector in parkinsonian monkeys; *in vivo* detection of gene expression and restoration of dopaminergic function using pro-drug approach. *Exp Neurol* **164**: 2–14.
10. Bobo, RH, Laske, DW, Akbasak, A, Morrison, PF, Dedrick, RL and Oldfield, EH (1994). Convection-enhanced delivery of macromolecules in the brain. *Proc Natl Acad Sci USA* **91**: 2076–2080.
11. Bartlett, JS, Samulski, RJ and McCown, TJ (1998). Selective and rapid uptake of adeno-associated virus type 2 in brain. *Hum Gene Ther* **9**: 1181–1186.
12. Ciesielska, A, Mittermeyer, G, Hadaczek, P, Kells, AP, Forsayeth, J and Bankiewicz, KS (2009). Anterograde axonal transport of AAV2-GDNF in rat basal ganglia. *Molecular Therapy*: 1–6.
13. Samaranch, L, Salegio, EA, San Sebastian, W, Kells, AP, Bringas, JR, Forsayeth, J *et al.* (2013). Strong cortical and spinal cord transduction after AAV7 and AAV9 delivery into the cerebrospinal fluid of nonhuman primates. *Hum Gene Ther* **24**: 526–532.
14. Barski, JJ, Hartmann, J, Rose, CR, Hoebeek, F, Mörl, K, Noll-Hussong, M *et al.* (2003). Calbindin in cerebellar Purkinje cells is a critical determinant of the precision of motor coordination. *J Neurosci* **23**: 3469–3477.
15. Aalbers, CJ, Tak, PP and Vervoordeldonk, MJ (2011). Advancements in adeno-associated viral gene therapy approaches: exploring a new horizon. *F1000 Med Rep* **3**: 17.
16. Manning, WC, Zhou, S, Bland, MP, Escobedo, JA and Dwarki, V (1998). Transient immunosuppression allows transgene expression following readministration of adeno-associated viral vectors. *Hum Gene Ther* **9**: 477–485.
17. Treleaven, CM, Tamsett, TJ, Bu, J, Fidler, JA, Sardi, SP, Hurlbut, GD *et al.* (2012). Gene transfer to the CNS is efficacious in immune-primed mice harboring physiologically relevant titers of anti-AAV antibodies. *Mol Ther* **20**: 1713–1723.
18. Dodiya, HB, Bjorklund, T, Stansell, J 3rd, Mandel, RJ, Kirik, D and Kordower, JH (2010). Differential transduction following basal ganglia administration of distinct pseudotyped AAV capsid serotypes in nonhuman primates. *Mol Ther* **18**: 579–587.
19. McBride, JL, Pitzer, MR, Boudreau, RL, Dufour, B, Hobbs, T, Ojeda, SR *et al.* (2011). Preclinical safety of RNAi-mediated HTT suppression in the rhesus macaque as a potential therapy for Huntington's disease. *Mol Ther* **19**: 2152–2162.
20. Klein, RL, Dayton, RD, Leidenheimer, NJ, Jansen, K, Golde, TE and Zweig, RM (2006). Efficient neuronal gene transfer with AAV8 leads to neurotoxic levels of tau or green fluorescent proteins. *Mol Ther* **13**: 517–527.
21. Gray, SJ, Foti, SB, Schwartz, JW, Bachaboina, L, Taylor-Blake, B, Coleman, J *et al.* (2011). Optimizing promoters for recombinant adeno-associated virus-mediated gene expression in the peripheral and central nervous system using self-complementary vectors. *Hum Gene Ther* **22**: 1143–1153.
22. Bevan, AK, Duque, S, Foust, KD, Morales, PR, Braun, L, Schmelzer, L *et al.* (2011). Systemic gene delivery in large species for targeting spinal cord, brain, and peripheral tissues for pediatric disorders. *Mol Ther* **19**: 1971–1980.
23. Matsushita, T, Elliger, S, Elliger, C, Podsakoff, G, Villarreal, L, Kurtzman, GJ *et al.* (1998). Adeno-associated virus vectors can be efficiently produced without helper virus. *Gene Ther* **5**: 938–945.
24. Wright, JF, Qu, G, Tang, C and Sommer, JM (2003). Recombinant adeno-associated virus: formulation challenges and strategies for a gene therapy vector. *Curr Opin Drug Discov Devel* **6**: 174–178.
25. Fiandaca, MS, Forsayeth, JR, Dickinson, PJ and Bankiewicz, KS (2008). Image-guided convection-enhanced delivery platform in the treatment of neurological diseases. *Neurotherapeutics* **5**: 123–127.
26. Krauze, MT, Saito, R, Noble, C, Tamas, M, Bringas, J, Park, JW *et al.* (2005). Reflux-free cannula for convection-enhanced high-speed delivery of therapeutic agents. *J Neurosurg* **103**: 923–929.